NREL/CP-500-24920 • UC Category: 1213

Modeling, Testing and Economic Analysis of a Wind-Electric Battery Charging Station

Vahan Gevorgian, David A. Corbus,
Stephen Drouilhet, Richard Holz
National Renewable Energy Laboratory

Karen E. Thomas
University of California at Berkeley

Presented at
Windpower '98
Bakersfield, CA
April 27-May 1, 1998

National Renewable Energy Laboratory
1617 Cole Boulevard
Golden, Colorado 80401-3393
A national laboratory of the U.S. Department of Energy
Managed by Midwest Research Institute
for the U.S. Department of Energy
under contract No. DE-AC36-83CH10093

Work performed under task number WE802230

July 1998

NOTICE

Available to DOE and DOE contractors from:
Office of Scientific and Technical Information (OSTI)
P.O. Box 62
Oak Ridge, TN 37831
Prices available by calling (423) 576-8401

Available to the public from:
National Technical Information Service (NTIS)
U.S. Department of Commerce
5285 Port Royal Road
Springfield, VA 22161
(703) 487-4650

Printed on paper containing at least 50% wastepaper, including 20% postconsumer waste

MODELING, TESTING, AND ECONOMIC ANALYSIS OF A WIND-ELECTRIC BATTERY CHARGING STATION

Vahan Gevorgian, David A. Corbus, Stephen Drouilhet, Richard Holz
National Wind Technology Center
National Renewable Energy Laboratory
1617 Cole Blvd., Golden, CO 80401 USA

Karen E. Thomas
Department of Chemical Engineering
University of California at Berkeley
Berkeley, CA 94720 USA

ABSTRACT

Battery charging systems are very important in many developing countries where rural families cannot afford a solar-battery home system or other electricity options, but they can afford to own a battery (in some cases more than one battery) and can pay for it to be charged on a regular basis. Because the typical households that use batteries are located far from the grid, small wind battery charging stations can be a cost-competitive option for charging batteries. However, the technical aspects of charging numerous 12-volt batteries on one DC bus with a small permanent magnet alternator wind turbine suggest that a special battery charging station be developed.

NREL conducted research on two different types of wind battery charging stations: a system that uses one charge controller for the entire DC bus and charges batteries in parallel strings of four batteries each, and one that uses individual charge controllers for each battery. We present test results for both system configurations. In addition, modeling results of steady-state time series simulations of both systems are compared. Although the system with the single charge controller for the entire bus is less expensive, it results in less efficient battery charging. We also include in the paper a discussion of control strategies to improve system performance and an economic comparison of the two alternative system architectures.

INTRODUCTION

A conventional lead-acid car battery still appears to be a cheap and reliable source of electrical power for small household applications for many parts of the developing countries (remote communities, islands, etc.). Even the small amount of energy (~1 kWh) that these battery store can sufficiently improve the quality of life for such areas, thereby giving people access to electrical lighting, TV/radio, and other conveniences. It is a common practice for rural inhabitants in developing countries to acquire electrical service by charging 12-volt, 50-100 amp-hour batteries from diesel-powered grids. The major advantage of a centralized battery-charging station is that it can bring electric service to a very low-income segment of the population. The use of wind-electric battery charging stations represents an alternative to conventional diesel-powered stations in many developing countries of the world. To date, there have been only a few examples of renewable-based battery charging stations, mostly using photovoltaics (PV). Although the design of a wind-powered battery charging station can be more complex (because of the nature of the wind resource), wind-powered stations offer greater economy of scale than do PV stations. The studies conducted at NREL identified a market for a wind-electric battery charging station that

- Provides a fast charge yet protects the batteries
- Accepts batteries of various capacities
- Has high reliability and is simple to operate
- Is cost effective and viable in terms of logistic and operational issues.

Modeling and testing activities at NREL on wind-powered battery charging stations focused on a low-cost method for charging 12-volt deep cycle lead-acid batteries from a small wind turbine (e.g., 10 kW). Two system alternatives were evaluated: 1) strings of batteries connected to a common DC bus and voltage control for the entire DC bus (existing commercial system), 2) individual charge controllers used for each battery. The major goal of this paper is to model and analyze the system and to predict the performance improvements that can be achieved by altering the system configuration. It will discuss the primary aspects of the two system configurations based on modeling and testing results.

TWO SYSTEM ARCHITECTURES

The main technical challenge in the design of a wind-electric battery charging station is to come up with a system configuration and control algorithm that maximizes wind energy production from the turbine and also provides favorable charging conditions for batteries. This task is complex because of the variability of the wind: continual wind speed variations result in varying wind turbine power output. Ideally, the system configuration and its controller should optimize the match between the wind rotor and load, thereby allowing the maximum available power from the wind to be used, while at the same time charging the batteries with an optimum (for a given type of battery) charge profile. This will maximize the number of batteries charged by a station within a certain time period.

The configuration with a single charge controller requires the operator to group batteries into parallel strings (Fig. 1), with batteries in the same string at the same capacity and initial state of charge (SOC). Otherwise, a battery with a higher initial SOC would get charged faster and start gassing while the rest of the batteries in the string remain undercharged. So a procedure for reliable SOC determination (assuming similar battery brand, aging of the batteries, etc.) is required for this configuration. This configuration also has certain performance limitations [1]. The inherent electrical characteristics of a permanent magnet generator result in a poor match between a standard rectifier/battery combination and a wind turbine generator. Both low- and high-wind performance suffer as a result of the impedance mismatch between the generator and the load [2]. At low wind speeds, and therefore low generator frequency, the generator has a low source impedance and the rectifier/battery combination has very high impedance (no current will flow until the rectified generator voltage exceeds the battery voltage). At high wind speeds, and high generator frequency, the generator source impedance is high (resulting from its internal inductance and resistance), while the battery impedance is quite low (i.e., small changes in charging voltage cause large changes in current).

One way to improve generator performance is to change the apparent DC bus voltage seen by the generator. This can be achieved by various methods. In this paper, we propose to have DC-DC converters inserted between the DC bus and each individual battery (Fig. 1). The input DC voltage of the converters varies over a wide range depending on generator frequency and total power to the batteries. The output voltage of each individual converter is determined by the battery SOC. The current output of the individ-

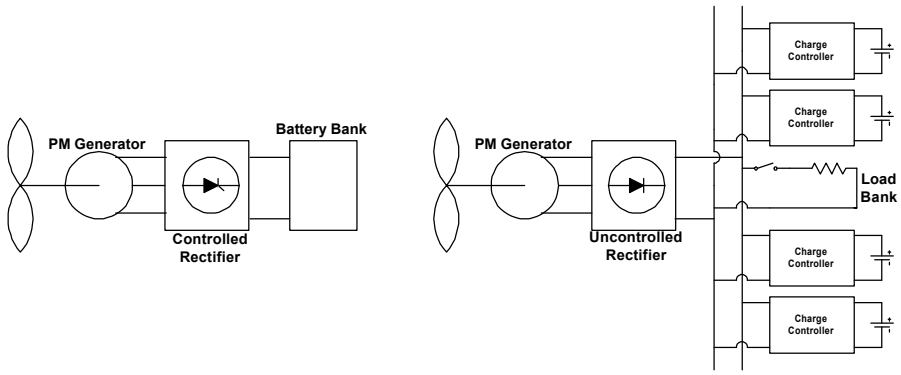

FIGURE 1: TWO BATTERY CHARGING CONCEPTS

ual converters can be controlled, allowing control of total power to the battery bank and providing the desired charge profile for a battery. When the battery voltage reaches some preset value, the converter starts to limit current to protect the battery. By controlling the total current flow to the battery bank, a better match between the generator and load is achieved. This load matching control algorithm is generically known as maximum power point tracking. In order to protect the converters from overvoltage on their input side, a switched load bank or controlled rectifier can be used.

DESCRIPTION OF THE SYSTEM MODEL

In order to compare the long-term performance of both system architectures, we developed a steady-state model of a wind-electric battery charging station. The model can be separated into AC and DC portions. The AC portion of the model includes a three-phase permanent magnet synchronous generator and rectifier connected to a DC bus. A wind turbine rotor drives the generator's shaft. The wind rotor is modeled by its power coefficient C_p versus tip-speed-ratio (TSR) curve. The generator is modeled as a frequency-proportional AC voltage source in series with an inductance and resistance. The rectifier is presented to be a purely sinusoidal voltage source with unity power factor, and the generator's AC terminal voltage is in direct proportion with the rectifier's DC side voltage. The schematic and steady-state equations for these components were presented in previous papers [1,2]. For the purposes of this work, this portion of the model was supplemented only by the equations for a three-phase transformer, which in actual systems is usually inserted between the generator and rectifier.

The DC portion of the model consists of a main DC bus connected to many individual batteries either directly or through individual controlled-current DC-DC converters. The battery model used in this analysis is similar to models presented previously[3,4]. The battery is viewed as a DC voltage source in series with a nonlinear resistance, which represents the internal resistance of the battery (Fig. 2). The battery open circuit voltage (OCV) and internal resistance are represented as a function of charge (Ah) delivered into the battery. Voltage across the battery terminals can be calculated easily using a charging current and Ah delivered to a battery:

$$U_{bat}(I_{bat}, Q) = I_{bat} R_{\text{int}}(Q) + E_{oc}(Q) \tag{1}$$

The measured open-circuit voltage (OCV) for the Trojan 24 EV deep discharge 12-volt/85 Ah lead-acid batteries was used in the analysis. This voltage differs from the "at rest" OCV (i.e., voltage when the battery has not been charged for a significant period of time). It was measured instantaneously after the battery was disconnected from the voltage source periodically during the charging process. The battery internal resistance was calculated using the OCV, current, and terminal voltage measurements. This battery model is valid for the charge mode only. The model does not take into account battery and ambient temperatures. Incorporating these temperatures into the model will improve its accuracy. However, accurate battery simulation was not the main objective of this work. The battery model is used to compare two battery charging architectures.

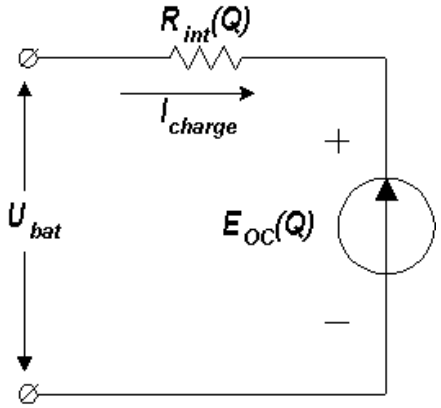

FIGURE 2: BATTERY ELECTRICAL SCHEMATIC

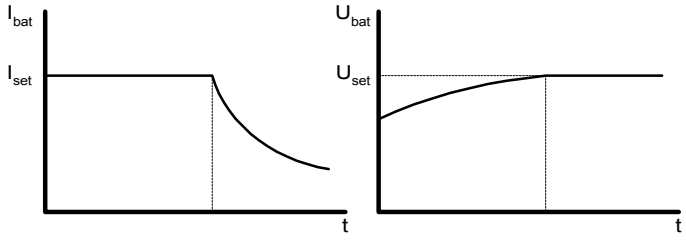

FIGURE 3. IDEAL CHARGE PROFILE FOR INDIVIDUAL CHARGE CONTROLLER

For a system with individual charge controllers, the power to each individual battery can be calculated easily using Equation (1). The individual charge controllers can be simulated by their charge profiles. The ideal charge profile for a battery is represented in Fig. 3. The charging process consists of two stages: constant current and constant voltage charge. Both constant current I_{set} and voltage U_{set} settings can be set as desired depending on the battery type.

A battery bank of m parallel strings with n batteries in each string can be modeled assuming that batteries in the same string are of similar charge Q_i. Current to each individual string I_i and total current I_{tot} to the battery bank are given by

$$I_i = \frac{U_{dc} - nE_{oc}(Q_i)}{nR_{\text{int}}(Q_i)} \qquad I_{tot} = \sum_{i=1}^{m} I_i \tag{2}$$

Power to the battery bank can be found as follows (Q – is a vector of charges delivered to each string)

$$P_{bat.bank}(U_{dc}, \vec{Q}) = \sum_{i=1}^{m} \frac{U_{dc}^2 - nU_{dc}E_{oc}(Q_i)}{nR_{\text{int}}(Q_i)} \qquad \vec{Q} = [Q_1, Q_2 \ldots Q_m]^T \tag{3}$$

For steady-state simulation the solid-state charge control devices can be implemented into the model by using their logical functions. The overvoltage protection, current limiting, and various charge profiles can be modeled numerically with a set of "IF" statements incorporated into the model. The controlled rectifier for the system with a common DC bus can be modeled using the preset voltage value when the rectifier goes into a current limiting mode. Charge profiles for individual charge controllers can be also implemented using the same approach.

An iterative algorithm was developed to simulate numerically battery charging station performance for both system architectures using given wind speed time series. The system's power balance equations are solved numerically within each iteration loop for DC bus voltage and generator frequency f. It is assumed that the wind speed and charge of each individual battery or string of batteries remains constant within each iteration loop. The power to each individual battery or to each string of batteries is calculated based on the DC bus voltage and the SOC of the batteries. Various conditions corresponding to given control settings are checked within each iteration loop. The battery replacement event occurs when an individual battery or battery string reaches full SOC. Some modeling results are presented in the following section.

TESTING OF A 10-kW WIND TURBINE IN A BATTERY CHARGING STATION APPLICATION

The tested system diagram is shown in Fig. 4. The 10-kW Bergey wind turbine system is connected to the 48 VDC battery bank that consists of 16 Trojan 24 EV deep discharge 12-volt lead-acid batteries connected in four parallel strings. Rated capacity of each battery is 85Ah@20 hr and 55 Ah@2 hr charge rate. The generator is a three-phase permanent magnet (PM) alternator with 38 poles. Power to the battery bank depends on the wind speed and the state of charge of the battery bank. The rectifier control is used only to protect batteries from an overvoltage condition. When the battery voltage reaches a preset level, the voltage control system (VCS) limits the DC bus current thus avoiding battery overcharge. The three-phase 30

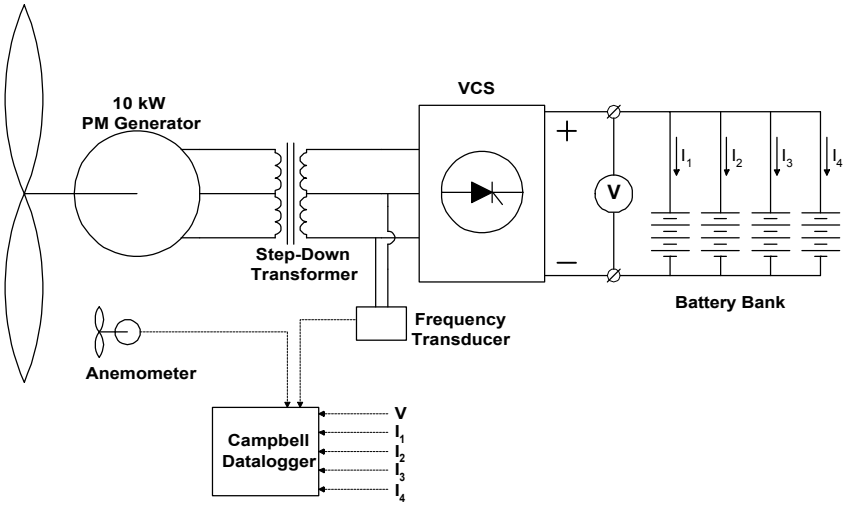

FIGURE 4. TEST SET-UP FOR 10-KW WIND TURBINE SYSTEM

kVA step-down (2:1) transformer is used to reduce the generator output voltage. Our primary finding from the testing is that battery strings at similar SOC tend to converge (low SOC strings absorb more of the current, so they "catch up" to the others), which leads to a batch process and poor overall efficiency.

Figure 5 shows the consolidated data on wind speed and DC power measurements for several tests at 30%–50% state of charge of the battery bank. The DC power output of the wind turbine generator is limited at about 5 kW although it is supposed to go as high as 6–6.5 kW for a battery charging application. This can be explained by the fact that only four parallel strings of batteries were used in the test. The higher current in the beginning of the charge causes fast build up of battery voltage. It limits the power into a battery at a certain level. The cut-in wind speed is about 4 meters/second (m/s). At about 10 m/s wind speed the power curve reaches the 5-kW power level. It stays at that level with further wind speed increases.

The following limitations and operational issues were exposed during the testing process:

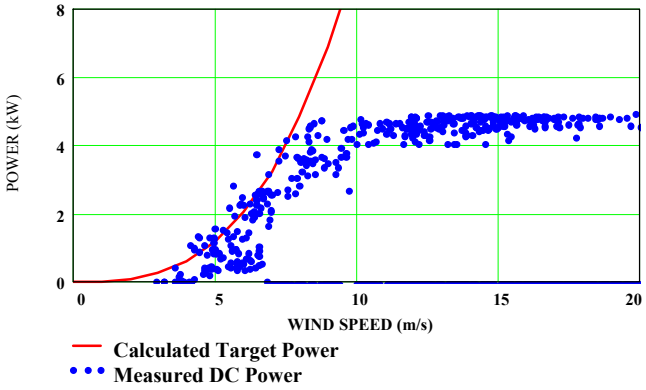

FIGURE 5. DC POWER VERSUS WIND SPEED

1. As mentioned earlier, the batch mode operation causes certain limitations to the system's efficiency because of the fact that the strings with a lower initial state of charge draw more current in the beginning. As a result, the whole battery bank approaches 100% SOC at about same time. The system efficiency decreases significantly at the end of the charging process even if there is enough power in the wind to run the system at rated power. It also causes longer overall charging time.
2. The batteries of similar initial state of charge and same capacity must be grouped in each string. This procedure is time consuming and requires accurate determination of the state of charge for each battery by measuring its specific gravity. This will cause problems in a real battery charging station where batteries of various brands and ages might be used.
3. The VCS used in the test set-up has a simple and reliable design. However, when operating in real conditions, any damage to the VCS circuit would cause station shutdown.

COMPARISON OF TEST AND MODELING RESULTS

We used the data obtained from system test runs to validate the model. Fig. 7 shows the comparison of calculations and measurements for the wind turbine DC power output. The measured wind speed is shown in Fig. 6. There was a one-minute time interval between measurements. The average wind speed was 5.4 m/s. The model was run using the same wind data file and the initial state of charge of the battery bank for this test was about 40%.

The comparison of test and modeling results for this and other tests shows acceptable agreement. The model calculates steady-state frequencies at each iteration step and uses its value to calculate the power. It means that the wind rotor equations incorporated into the model are correct. Some divergence between measured and calculated power, in particular at the end of the test, are explained by the fact that the model assumes that batteries in the same string are absolutely similar. However, in reality there is always some difference in behavior of each battery in the same string.

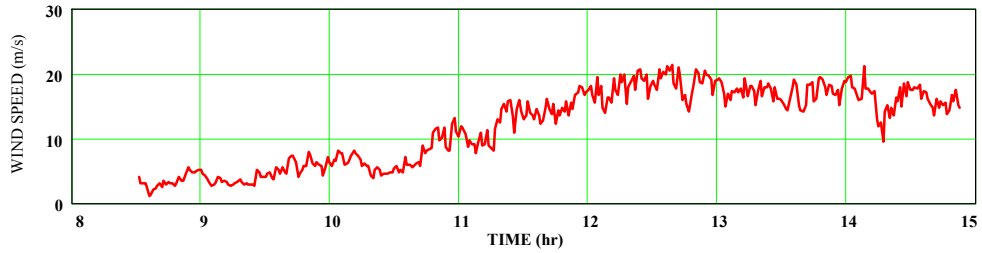

FIGURE 6. MEASURED WIND SPEED

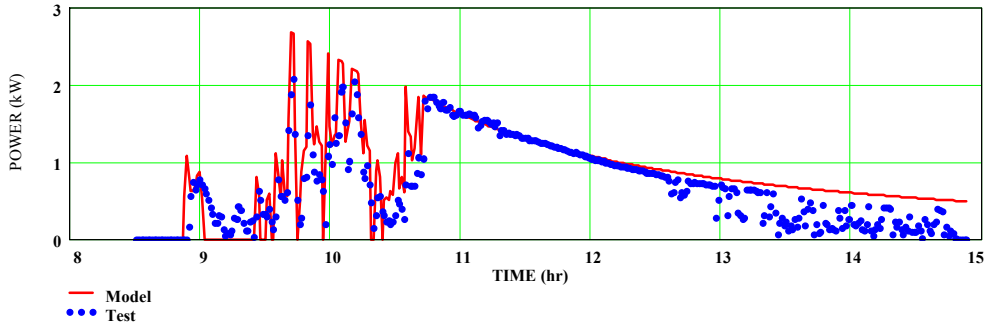

FIGURE 7. MODELED AND MEASURED POWER TO BATTERY BANK

TESTING OF PROTOTYPE SYSTEM WITH INDIVIDUAL CHARGE CONTROLLERS

The diagram of the system we tested is shown in Fig. 8. A 12-kW permanent magnet generator driven by a 75-kW DC motor was used as a power source. The output of the three-phase rectifier is connected to a DC bus with 16 Vicor DC-DC converters. Each converter is rated for 100 watts. The rated input DC voltage range of the converters is 100-300 VDC. Converters maintain 8 A constant charging current on the output. When the battery voltage reaches some preset level the converter starts to limit the current to a battery, thereby avoiding battery overcharge. So despite the wide variation of the input voltage (DC bus voltage) the converter is able to provide a good charge profile for the battery. Individual converters are switched on and off using the pulse signal supplied by a Labview control system to a Gate In pin of the converter. The Labview system also controls a dump load (5.2 ohm, 3 kW) switch in order to limit the DC bus voltage. The Labview DAQ board acquires analog signals from various sensors.

The main advantage of this configuration is that the DC bus voltage is "allowed" to vary across a wide range as opposed to being constrained by a directly connected battery bank. This additional degree of freedom, along with the possibility of controlling the number of active converters, is crucial to optimizing the system performance. Thus, this system configuration is capable of approximate maximum power point tracking. The wind rotor target power can be tracked by switching on a certain number of converters at a given alternator frequency, although the tracking resolution is limited to the power rating of a single converter (100 W for the tested system).

The peak power tracking precision can be improved significantly if, instead of switching converters on and off, there is a possibility to control simultaneously the output current of all converters in the system. In fact, the Vicor Corporation manufactures such converters rated for 200 watts. However, the higher input voltage range (200–400 VDC) will increase the cut-in frequency (and consequently the cut-in wind speed). So we decided to use the 100 watt Vicor DC-DC converters for this stage of the project .
The test results for the above system configuration are shown in Fig. 9. All 16 batteries during this test

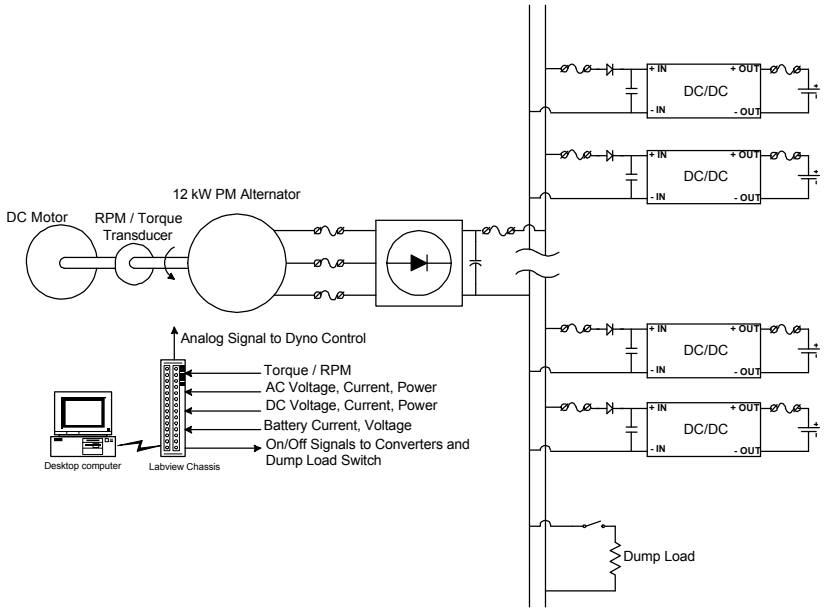

FIGURE 8. DYNAMOMETER TEST SET-UP OF THE PROTOTYPE BATTERY CHARGING STATION WITH INDIVIDUAL CHARGE CONTROLLERS

were at about 20% state of charge. The Labview control system starts switching converters on at the frequency of about 18 Hz when the DC bus voltage is within the converter's operational range of 100–300 VDC. Voltage keeps increasing almost linearly with the frequency. The number of activated converters increases as well. Each subsequent converter is switched on at the frequency determined by the Labview control program in a manner that the target power tracking is provided. When all 16 converters are on, the DC power does not increase any more with the frequency and stays at the level of 1.6 kW. The DC bus voltage, however, keeps increasing until it reaches the level of 300 VDC. At this point Labview activates the dump load to decrease the voltage and protect the converters. It appears that with a larger number of converters, this system could track the target power to much higher power levels.

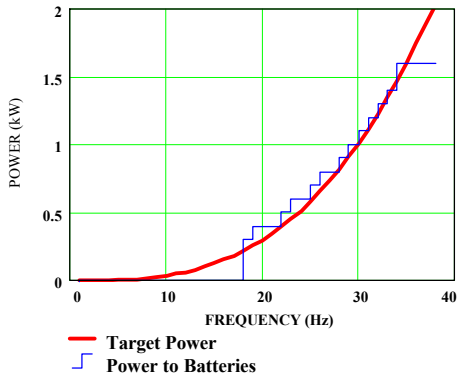

FIGURE 9. TARGET AND MEASURED POWER

As mentioned above, the peak power tracking could be more precise if it was possible to control the output current level of the converters. In this case, instead of step changes (as shown in Fig.18), the system output power would continuously follow the wind rotor target power.

ECONOMIC ANALYSIS OF WIND-ELECTRIC BATTERY CHARGING STATIONS

We compared the economics of the two charging systems based on the performance simulations. The comparison serves two purposes. The first is to determine which system is more cost effective. The second is to examine sensitivities to different economic parameters. Because parameters will vary widely depending upon the location in which the battery charging station is installed, it is important to understand the possible range of the parameters and how this variability affects the economics. Model simulations were run using thirty days of actual wind speed data for Xcalac, Mexico, (Fig.10) and assuming that the station operator "sleeps" 8 hours per day. If the battery reaches full charge during one of those "sleep" hours, then no battery replacement takes place. Upon reaching full charge during "waking" hours, a battery is immediately replaced with a completely discharged one.

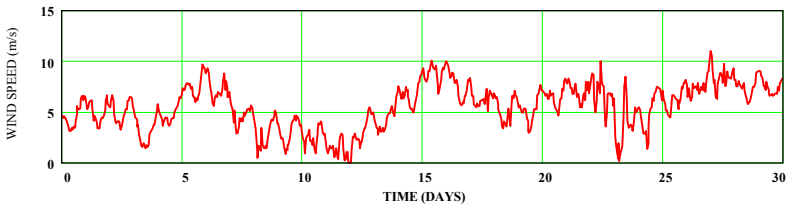

FIGURE 10. MEASURED WIND SPEED

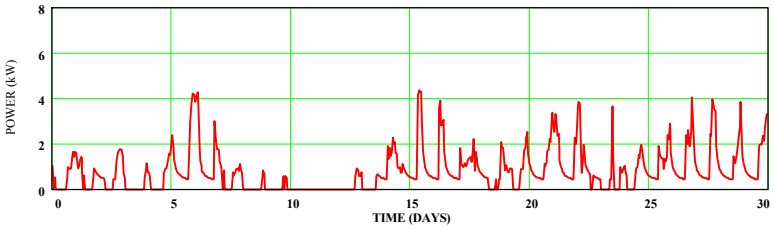

FIGURE 11. POWER TO BATTERY BANK FOR THE SYSTEM WITH VCS

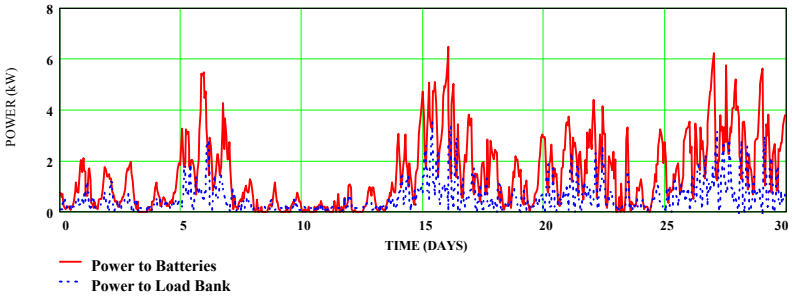

FIGURE 12. POWER TO THE BATTERY BANK AND DUMP LOAD FOR THE SYSTEM WITH INDIVIDUAL CHARGE CONTROLLERS

Results of a single run of the model are shown on Fig. 11 and 12 (average wind speed–5.5 m/s). The system with VCS consists of 8 parallel strings with 4 batteries per string (48 VDC system). The system with individual charge controllers consists of 32 DC-DC converters with dump load. The energy output and number of batteries charged for both configurations over the simulation period were calculated. The results for this and other runs are discussed further in this section

A standard lifecycle cost and net present value analysis was used. Capital and operation and maintenance (O&M) costs are shown in Table 1. Wind turbine costs are based on manufacturer's estimates for a Bergey Excel 10-kW turbine. Installation costs are estimated and will vary depending upon location, but such variability was not analyzed here. Installation costs are higher for the VCS system because of the added expense of installing the transformer for the charging station. The battery charging station costs are divided into fixed and variable. The variable costs depend on how many batteries the charging station can charge at a time; i.e., how many charging "ports" it has. Fixed costs for the VCS system are based on

manufacturer's estimates. For the DC-DC system, costs are estimated based upon the prototype built at the NWTC. The variable costs for the DC-DC system consist of the cost of the individual DC-DC converters, while for the VCS system the variable costs consist of added balance of system wiring, etc. The 25- year average design life was used in the calculations.

TABLE 1. CAPITAL AND O&M COSTS

Cost	**VCS System**	**DC-DC System**
Capital Costs		
Wind turbine		
Turbine ($)	21,000	21,000
Installation ($)	7,000	5,000
Battery charging station		
Fixed costs ($)	3,800	6,429
Variable costs ($/port)	16	194
O&M Costs		
Turbine and station maintenance ($/kWh)	0.05 (0.04 - 0.10)	0.10 (0.04-0.10)
Operator salary ($/year)	2,000 (0 - 10,000)	2,000 (0 - 10,000)

Expected values of O&M costs are shown in Table 1 with expected ranges in parentheses. Maintenance costs, as a function of kilowatt-hours (kWh) into the batteries per year (as predicted by the performance simulations), are based on field experience with Excel turbines. Maintenance costs are assumed to be higher for the DC-DC system because of its added complexity and to account for periodic replacement of DC-DC converters. Operator salary will of course depend highly on the location of the station. It is included because of its large effect on the economics.

Performance parameters evaluated were wind speed and the number of ports. Base case model simulations were run using 30 days of wind speed data from Xcalac, Mexico, which had an average wind speed of 5.5 m/s. The sensitivity of performance to wind speed was examined by linearly scaling the wind speed data to 6.5 and 4.5 m/s averages. The optimal number of ports was found to be 32 (that is, 32 DC-DC converters or eight strings of 4 batteries for the VCS system), and this was used as the base case value. Simulations were also run using 16, 24, and 40 ports. Simulation results are shown below.

TABLE 2. EFFECT OF WIND SPEED AND NUMBER OF PORTS ON PERFORMANCEDURING 30 DAY SIMULATION PERIOD

	DC-DC System		**VCS System**	
	No. batteries charged	Total kWh into batteries	No. batteries charged	Total kWh into batteries
Wind speed (with 32 ports)				
4.5 m/s	608	736.0	320	392.7
5.5 m/s	993	1200.0	576	671.6
6.5 m/s	1393	1762.0	608	778.4
Number of ports (at 5.5 m/s wind speed)				
16 ports	831	1017.0	304	473.7
24 ports	957	1157.0	432	502.2
32 ports	993	1200.0	576	671.6
40 ports	994	1200.0	560	638.7

Table 3 shows the base case and range of the net present value and lifecycle cost (cost per charged battery) for the two charging architectures. The base case uses the expected average values of the economic and performance parameters, while the range was found from "best case" and "worst case" scenarios, in which the expected least-cost and highest-cost values of all parameters, respectively, were used. The VCS system

cost clearly has a lower net present value, because the capital cost and maintenance of the charging station is less. However, because the DC-DC system charges approximately 60% more batteries than the system with VCS, the DC-DC system has a 25% lower lifecycle cost.

TABLE 3. AVERAGE AND RANGE OF NET PRESENT VALUE AND COST PER CHARGED BATTERY

	Net present value of capital and O&M costs	Cost per charged battery
DC-DC system	$68,042 (42,049 - 83,856)	$0.27 (0.08 - 4.53)
VCS system	$53,606 (33,813 - 76,629)	$0.36 (0.15 - 7.87)

CONCLUSIONS/FUTURE PLANS

A steady-state model of a wind-electric battery charging station was developed for two basic system configurations. We tested the Bergey 10-kW wind turbine system with VCS at the NWTC in a battery charging station application. Certain operational limitations for battery charging station application were revealed during the testing. The "proof-of-concept" system with individual charge controllers was developed and tested using the dynamometer set-up at the NWTC. The comparative economic analysis of both system configurations based on steady-state modeling was carried out. It demonstrated the superiority of the system with individual charge controllers over the system with VCS in terms of average number of batteries charged over a certain period of time. This performance improvement comes at higher system capital cost. However, the cost per charged battery of the system with individual charge controllers is lower because of better performance characteristics.

A prototype commercial version of the wind-electric battery charging station with individual charge controllers is being developed under the NREL subcontract. The system's design and control features have been developed based on the results of this work. The prototype commercial version will be tested at NWTC by late 1998.

ACKNOWLEDGEMENTS

Special thanks to Brian Gregory, Rick Holz, Eduard Muljadi, Ian Baring-Gould and Jonathon Touryan for their outstanding contributions to the modeling, hardware development, and testing stages of this work. This paper was written at the National Renewable Energy Laboratory in support of the U.S. Department of Energy under contract number DE-AC36-83CH10093.

REFERENCES

[1] E. Muljadi, S. Drouilhet, R. Holz, V. Gevorgian, "Analysis of wind power for battery charging." NREL/TP-441-8170. Presented at 15th ASME Wind Energy Symposium, Houston, TX, Jan. 28–Feb. 2, 1996

[2] S.Drouilhet, E. Muljadi, R. Holz, V. Gevorgian, "Optimizing small wind turbine performance in battery charging applications." NREL/TP-441-7808. Presented at Windpower '95, Washington, DC, March 26–30, 1995.

[3] J.F. Manwell, J.G. McGowan, "Lead acid battery storage model for hybrid energy systems." Solar Energy, Volume: 50:5, May 1993, Page 399–405.

[4] T.R. Morgan, R.H. Marshall, B.J. Brinkworth, "Modeling the resistance characteristics of the lead acid storage battery." Solar Energy Unit, School of Engineering, University of Wales, Cardiff, UK.